Combined Influence of Inorganics and Transport Limitations on the Pyrolytic Behaviour of Woody Biomass

Hernán Almuina-Villar[a,*], Peter Sommersacher[b], Stefan Retschitzegger[b], Andrés Anca-Couce[c] , Alba Dieguez-Alonso[a]

[a] Technische Universität Berlin, Institute of Energy Engineering, Seestr. 13 13353 Berlin, Germany
[b] BEST – Bioenergy and Sustainable Technologies GmbH, Inffeldgasse 21b, A-8010 Graz, Austria
[c] Technische Universität Graz, Institute of Thermal Engineering, Inffeldgasse 25B 8010 Graz, Austria
 h.almuinavillar@tu-berlin.de

A deeper understanding and quantification on the influence of inorganic species on the pyrolysis process, combined with the presence of heterogeneous secondary reactions, is pursued in this study. Both chemical controlled and transport limited regimes are considered. The former is achieved in a thermogravimetric analyser (TGA) with fine milled biomass in the mg range, while the latter is investigated in a particle level reactor with spherical particles of different sizes. To account for the influence of inorganics, wood particles were washed and doped with KCl aqueous solutions, resulting in K concentrations in the final wood of around 0.5% and 5% on dry basis. Gas species and condensable volatiles were measured online with Fourier transform infrared (FTIR) spectroscopy and a non-dispersive infrared (NDIR) gas analyzer. The removal of inorganic species delayed the pyrolysis reaction to higher temperatures and lowered char yields. The addition of inorganics (K) shifted the devolatilization process to lower temperatures, increased char and water yields, and reduced CO production among others. Higher heating rates and temperatures resulted in lower char, water, and light condensable yields, but significantly higher CH_4 and other light hydrocarbons, as well as CO. The increase in these yields can be attributed, at least in part, to the gas phase cracking reactions of the produced volatiles. Larger particle size increased the formation of char, CH_4 and other light hydrocarbons, and light condensables for low and high pyrolysis temperatures, while reduced the release of CO_2 and H_2O. This novel data set allows to quantify the influence of each parameter and can be used as basis for the development of detailed pyrolysis models which can include both the influence of inorganics and transport limitations when coupled into particle models.

1. Introduction and Objectives

The different reaction pathways during the pyrolysis process (pyrolysis mechanism) have a significant influence on products yields and composition, as well as on products properties relevant for their further application (Anca-Couce, 2016). Many studies have been performed to understand the relation between initial feedstock properties, pyrolysis conditions and products distribution and composition. Nevertheless, an accurate description of the pyrolysis mechanisms that can be globally applied is still missing due to the high degree of complexity of the reaction pathways involved and the numerous factors affecting their evolution (Anca-Couce, 2016; Anca-Couce et al., 2017). Alkali metals, with potassium being one of the most relevant, have been reported to play an important role on both devolatilization kinetics and products composition. Their catalytic effect in biomass results in a preference of the ring fragmentation reactions at the expense of sugar formation reactions (depolymerization, transglycoxylation) for both cellulose and hemicellulose. The former would lead to the formation of low molecular weight compounds and furan-ring derivatives, while the latter would lead mainly to levoglucosan and similar compounds (Patwardhan et al., 2010; Patwardhan et al., 2011; Trendewicz et al, 2015; LeBrech et al., 2016). The presence of alkali species may as well catalyse dehydration reactions at low temperature enhancing char formation (LeBrech et al., 2016; Trendewicz et al, 2015). For lignin pyrolysis, alkali species (Na) were shown to catalyse functional groups scission, favouring methanol release (demethoxylation) and dehydration reactions, as well as radicals recombination (Jakab et al., 1997). It was also shown

that alkali species (Na) catalysed functional groups cleavage in a selective manner, favouring demethoxylation over demethylation of guaiacyl units (Jakab et al., 1993). At the same time, the formation of CO and formalde-hyde was hindered, while decarboxylation and dehydration reactions were favoured (Jakab et al., 1993). Stud-ies in literature with similar approach as the present one also show that alkali species (K) during wood and other biomasses pyrolysis resulted in an overall increase of gas and char yields over liquid condensables (Hu et al., 2015; Shah et al, 2015, Di Blasi et al., 2018). Secondary charring reactions, i.e. further reactions of the primary volatiles within the solid/liquid matrix (and therefore triggered by transport limitations), have been shown to also influence products distribution and process thermochemistry (Lang et al., 2017; Almuina-Villar et al., 2019; Di Blasi et al., 2017; Anca-Couce et al., 2017; Di Blasi et al., 2018). Almuina-Villar et al. (2019) reported that the presence of K at slow pyrolysis led to a partially overlapped primary decomposition of cellu-lose and lignin, together with heterogeneous secondary reactions of primary volatiles, leading to higher exo-thermicity and formation of aromatic species, among other species. The present study constitutes an exten-sion of the work by Almuina-Villar et al. (2019), to investigate in detailed the combine action of inorganic spe-cies and heterogeneous reactions on the pyrolysis process. To this end, both chemical kinetic controlled (in-trinsic kinetics) and transport limited regimes at different conditions, including higher temperatures and inter-mediate heating rates, have been considered. The former is achieved in a thermogravimetric analyser (TGA) with fine milled biomass in the mg range, while the latter is investigated in a particle level reactor, with contin-uous monitoring of temperature and mass, using spherical particles of different sizes at different heating rates. To account for the influence of inorganics, wood particles were washed and doped with KCl aqueous solu-tions. Furthermore, gas species were characterized online, combining Fourier transform infrared (FTIR) spec-troscopy and non-dispersive infrared (NDIR) gas analyses. The data obtained in the present work, besides providing understanding on the combined influence of inorganics species and secondary charring reaction of the pyrolysis process can be also used as complete database for further modification of Ranzi´s detailed py-rolysis scheme, following the works by Trendewicz et al. (2015) and Anca-Couce et al. (2017) among others.

2. Experimental

Table 1: Properties for small (Ø = 6 mm) and big (Ø = 10 mm) particles.

Ø = 6 mm	Bw	Bw-H_2O	Bw-KCl_1	Bw-KCl_2
C (% wt., db)	48.57 ± 0.12	47.93 ± 0.11	46.90 ± 0.03	43.63 ± 0.12
H (% wt., db)	6.67 ± 0.03	6.63 ± 0.03	6.53 ± 0.02	6.01 ± 0.02
O* (% wt., db)	44.35 ± 0.15	45.16 ± 0.14	44.97 ± 0.04	41.03 ± 0.11
Inorg.(% wt.,db)	0.24 ± 0.01	0.16 ± 0.02	1.49 ± 0.02	9.21 ± 0.07
K (mg/kg)	708 ± 5	93 ± 8	7459 ± 185	47984 ± 852
Cl (mg/kg)	-	-	6790	43678
Ca (mg/kg)	1019 ± 46	958 ± 125	427 ± 15	177 ± 1
Ø = 10 mm	Bw	Bw-H_2O	Bw-KCl_1	Bw-KCl_2
Inorg.(% wt.,db)	0.25 ± 0.00	0.13 ± 0.00	1.07 ± 0.01	8.47 ± 0.09
K (mg/kg)	885 ± 4	199 ± 2	5243 ± 77	43612 ± 896
Cl (mg/kg)	-	-	4773	403801
Ca (mg/kg)	1032 ± 2	736 ± 3	843 ± 5	198 ± 15

The experimental setup used to perform the single particle pyrolysis experiments has been presented elsewhere (Sommersacher et al., 2015; Sommersacher et al., 2016; Anca-Couce et al., 2017). Beech wood spheres of two different sizes (Ø 10 mm and Ø 6 mm, referred as big and small particles, respective-ly) were used. Washed particles (referred as Bw-H_2O) were soaked in deionized water during 16 h in vacuum, dried 8h at 50 °C in vacu-um, and washed again under the same conditions. For KCl doped wood (referred as Bw-KCl_1 and Bw-KCl_2), the particles were, first washed, as for Bw-H_2O, and then soaked in different KCl aqueous solutions during 16 h in vacuum, resulting in K concentrations in the final wood of around 0.5 wt.% and 5 wt.%. Characterization of the materials is presented in Table 1. The single particle re-actor was preheated until 500°C and 900°C, in order to reach different heating rates and final temperatures in the particles. Detailed online characterization of the produced volatiles was achieved with a multi-component Fourier transform infrared (FTIR) spectroscopy system and with a non-dispersive infrared (NDIR) gas analyz-er. Mass and temperature evolution in the center and in the atmosphere around the particle were also charac-terized. A set of 3 experiments were performed for each case to ensure repeatability of the results. All the re-sults shown are an average of those measurements.

To study the chemical kinetics, milled samples from the big particles (Ø 10 mm) were prepared and afterwards measured in a thermogravimetric analyzer (TGA) in conditions that should ensure a chemical kinetic control regime, i.e. initial mass of around 10 mg and slow heating rates (10 °C/min). The results are shown as the de-rivative of the conversion ($d\alpha/dt$), being conversion (α) defined as $\alpha = (mi – m)/(mi – mf)$, where mi is the ini-tial mass of the particle, mf is the final char mass and m is the mass at each time step.

3. Experimental results

3.1 Chemical kinetic regime

The conversion rates ($d\alpha/dt$) of raw beech wood (Bw), washed beech wood (Bw-H_2O), and KCl-doped beech wood (Bw-KCl_1 and Bw-KCl_2) in TGA experiments are presented in Figure 1. Doping of wood with KCl significantly affected the pyrolysis chemistry, shifting to lower temperatures the maximum of the conversion rate and the shoulder attributed to the conversion of hemicellulose (Anca-Couce et al., 2016). Furthermore, the decay of the conversion rate (end of devolatilization process) was shifted as well to lower temperatures, leading to a reduced total devolatilization temperature span (and time). The shoulder at lower temperatures became less pronounced with higher K content as well. All together these results show the catalytic effect of K on the pyrolytic decompo-

Figure 1: Conversion rate ($d\alpha/dt$) obtained at 10 °C/min.

sition of biomass macrocomponents, hemicellulose, cellulose and lignin, leading to an increased overlap of the three regions with higher K content. These results are consistent with similar studies from literature (Shah et al., 2015). K-doping also increased the char yields, with values of 10.3 wt.%, 12.3 wt.%, 17.0 wt.%, and 25.5 wt.% at 700 °C (expressed on dry, additive free basis) for Bw-H_2O, Bw, Bw-KCl_1, and Bw-KCl_2, respectively.

3.2 Mass loss and temperature at particle level

The conversion rate at particle level is presented in Figure 2. Two particle sizes (Ø 6 mm and Ø 10 mm) were used to have differences in the potential influence of transport limitations on the pyrolysis process, including enhancement of heterogeneous secondary (charring) reactions. Furthermore, two pyrolysis temperatures (500 °C and 900 °C) were used, which led also to varying heating rates: approximately 300 °C/min and 1350 °C/min for small particles; and 215 °C/min and 900 °C/min for big particles. The addition of KCl also shifted the maximum of the conversion rate to slightly earlier times (and therefore lower temperatures) as for the chemical kinetic controlled (TGA) experiments. A narrowing of the devolatilization process with KCl doping was also observed for the experiments at 500 °C, as for the TGA
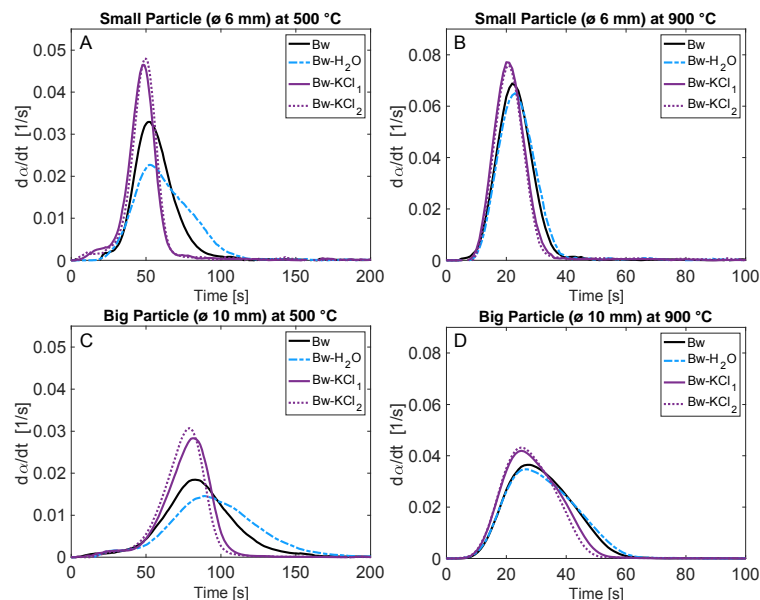

Figure 2: Conversion rate ($d\alpha/dt$) of: a) Small particles 500°C, b) Small particles 900°C, c) Big particles 500°C and d) Big particles 900°C.

measurements. However, at particle level it was also observed that the conversion rate curve for Bw-H_2O was notably wider than for Bw, extended in the temperature range associated to lignin decomposition. A similar behavior was also observed by Almuina-Villar et al. (2019) and attributed to the lack of catalytic effect on lignin pyrolysis upon removal of inorganics. Lower temperatures in the center of the particle during most of the devolatilization process for Bw-H_2O could also explain this delayed conversion at higher temperatures. However, the lower temperature at the center of the particle can only be explained by differences in the pyrolysis thermochemistry, since heat transfer outside and inside the particle should not vary for the same experimental conditions depending on K content.

In Figure 3 the different thermal regimes for the experiments previously introduced are presented with the dT/dt in the center of the particle (Di Blasi et al., 2017). It is possible to see clear differences between washed, raw, and KCl doped wood. For experiments at 500 °C several peaks are observed. The first one, after the particle heating, is attributed to hemicellulose and the last one to lignin (Figure 3, a). For Bw-KCl_1, and Bw-KCl_2, the peaks of dT/dt$_{particle}$ are larger, specially at the end of the conversion, showing a higher global exothermicity during the devolatilization process. This suggests that K also significantly affects the process thermochemistry, catalyzing exothermic reactions, including cellulose and lignin primary decomposition and secondary reactions of their primary products (Di Blasi et al., 2017; Almuina-Villar et al, 2019).
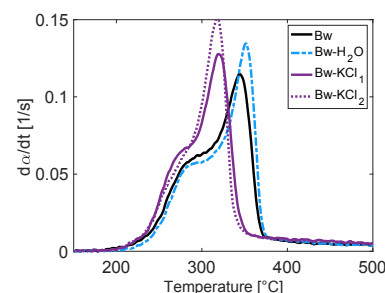
The last exothermic peak appears earlier (for Bw-KCl$_1$ and Bw-KCl$_2$) or delayed (Bw-H$_2$O) in comparison to Bw, in agreement with the conversion rate curves (Figure 2). For big particle size, the thermal regimes followed the same qualitative behavior as for small particle size for Bw. The last exothermic regime, attributed to lignin/lignin residue decomposition and secondary reactions, was significantly higher for Bw-KCl$_1$ and Bw-KCl$_2$, relative to other exothermic peaks, in comparison to the results for small particle size. This suggests that some of the reactions resulting in exothermicity may be also enhanced by the big particle size, i.e., potentially secondary reactions. In the experiments at 900 °C, the patterns for the four cases were very similar. Mainly a clear exothermic peak, coincident with lignin/lignin residue decomposition was observed. It is clear that K catalyzes

Figure 3: Rate of temperature increase (dT/dt) in the center of the particle for a) Small particle at 500°C, b) Small particle at 900°C, c) Big particle at 500°C and d) Big particle at 900°C

the wood devolatilization process, shifting it to lower temperatures and leading to an overlapping of the three macrocomponents decomposition. Furthermore, it catalyzes char formation, which has been reported in literature (e.g. Di Blasi et al., 2017) to be an exothermic process. However, looking at the thermochemistry of the process under the different studied conditions, the exothermic influence of K on the pyrolysis process is further enhanced by the presence of transport limitations, probably due to the occurrence of heterogeneous secondary reactions. This could be also understood as heterogeneous secondary reactions are favored by K doping. The fact is that both factors act combined and cannot be separated.

3.3 Yields at particle level

The product yields for both particle sizes and pyrolysis temperatures are plotted in Figure 4. With increasing pyrolysis temperature (500 °C versus 900 °C), the yields of CO, CH$_4$, and other light hydrocarbons (LH: ethene, acetylene, propane, propene) increased, while light condensable species (LC: acetic acid, lactic acid, formaldehyde, acetaldehyde, methanol, ethanol) and char yields decreased. CO$_2$ yields remained quite constant, with values of around 13–15 wt.% and H$_2$O decreased from around 15 wt.% to values in the range of 5-10 wt.%, depending on particle size. The decrease of char yields with higher pyrolysis temperatures (900 °C) can be explained by the higher heating rates achieved, which favor the yields of gas and condensable volatiles, as well as by further char reactions that can happen at high temperatures. The increase in CO, CH$_4$, and other LH can be explained by an increase in gas phase tar cracking reactions due to high temperatures.

Regarding inorganics, their presence in the initial feedstock has been reported to increase char and gas yields at the expense of condensable volatiles (Shah et al., 2015; Hu et al., 2015; Di Blasi et al., 2018). This is also observed in the present study, i.e. the higher the K content, the higher the char yields, due to catalysis of charring reactions, as previously discussed. It must be taken into account that this char yields include also the inorganics species remaining in the char after the pyrolysis process. The organic fraction of this char is lower than the plotted values. Nevertheless, the organic fraction of the char is also increased with higher K content. Bigger particle size also led to an increase in char yields for both pyrolysis temperatures. Therefore, the highest char yields were obtained with K doping and big particle size. Permanent gases (CO and CO$_2$) remained quite constant at low pyrolysis temperatures with the presence of inorganic species. Only a 1 wt.% decrease in CO for both particle sizes could be observed with the increase in K content. However, at 900 °C, CO production was drastically reduced along with a significant increase in H$_2$O and only a very slight increase in CO$_2$ with K loading. The inhibition in CO release at high temperatures with K doping has been also observed by Demirbaş (2002), who obtained similar results by adding K$_2$CO$_3$ to the initial feedstock and by Hu et al. (2015), who found that washing with H$_2$O and HCl resulted in higher CO yields at the expense of H$_2$ and CO$_2$. With respect to light condensable (LC) species, their yields were slightly increased by particle size and reduced by K content (slightly) and by high pyrolysis temperature (strongly). The latter can be attributed to secondary gas cracking reactions (Anca-Couce et al., 2017). In Figure 5, light condensables and CH$_4$ release for Bw-H$_2$O (a)

and Bw-KCl$_1$ (b), big particle size at 500 °C is presented. Upon addition of K, light condensables release was narrowed, in good agreement with the devolatilization behavior.
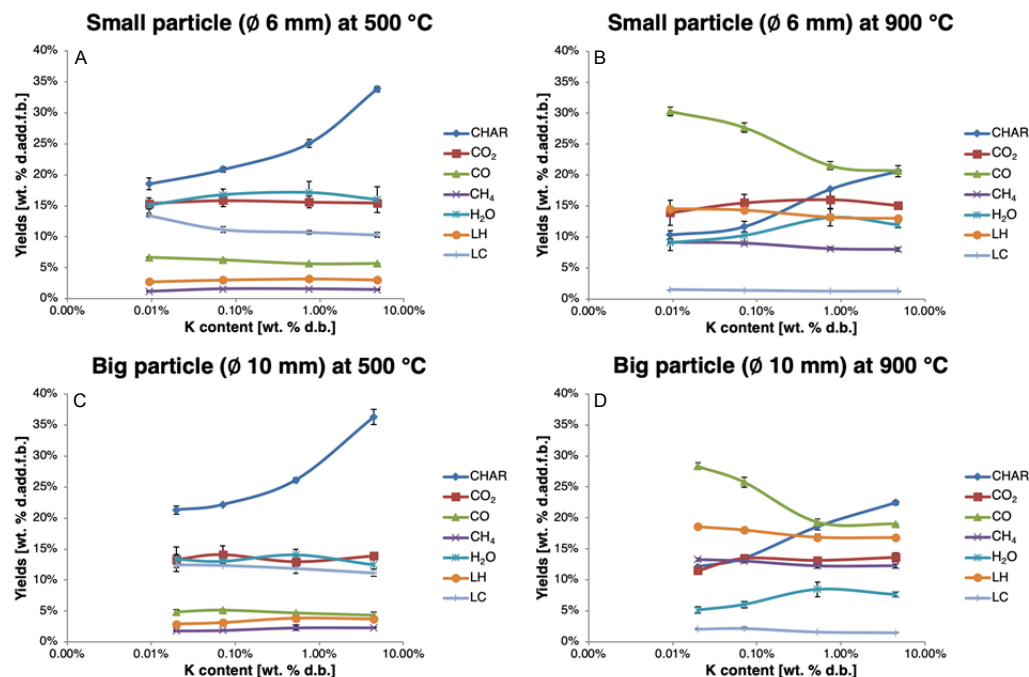

Figure 4: Product yields in dry additive (KCl) free basis with standard deviations for a) Small particle at 500°C, b) Small particle at 900°C, c) Big particle at 500°C and d) Big particle at 900°C
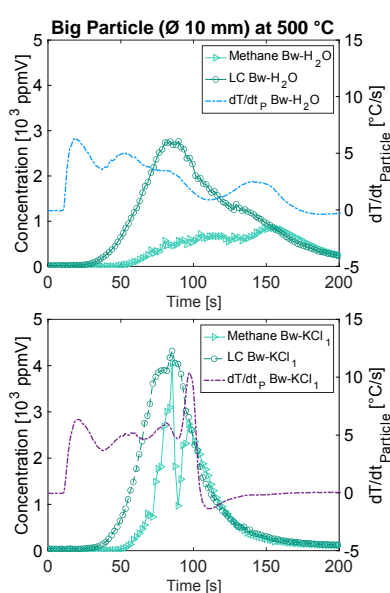

Figure 5: Methane and light condensables release together with dT/dt_P for a) Bw-H$_2$O and b) Bw- KCl$_1$

In the case of CH$_4$ at 500 °C, its formation seems to be slightly promoted with big particle size. At low pyrolysis temperatures, K doping did not significantly affect the total CH$_4$ yields. However, the time dependent release was strongly modified. In Figure 5 it is shown that for Bw-H$_2$O the main release of CH$_4$ was coincident with the final exothermic peak and attributed to lignin/lignin residue decomposition and secondary reactions of primary volatiles, as previously introduced. However, upon addition of K, CH$_4$ release increased significantly during the main devolatilization process. This indicates an enhancement of lignin reactivity and secondary reactions with the addition of K, potentially favored by bigger particle size. At 900 °C CH$_4$ decreased with K content. Other light hydrocarbons, such as ethene, acetylene and propane followed the same trend as CH$_4$ (results of single yields not shown). Jakab et al. (1997) discussed that Na doping reduced slightly the production of methane, while enhanced demethoxylation reactions, leading to methanol release. The formation of CH$_4$ would require not only the functional group cleavage, but also the availability of transferable H (Jakab et al., 1997) which as shown by Le Brech et al. (2016) is reduced with K doping. Furthermore, CH$_4$ yields were higher for big particle size than for small particle size, indicating the presence of other reactions within the solid matrix leading to the production of CH$_4$.

4. Conclusions

It has been shown and quantified the combined impact of K doping with the presence of secondary heterogeneous reactions (enhanced by higher transport limitations) on the pyrolysis process. Besides the known catalytic effect of K on charring reactions, leading to higher char and water yields, other relevant patterns have been as well identified and quantified, as it is the suppression of CO release, affected as well by the increased presence of transport limitations. CH$_4$ formation was observed to be reduced at high pyrolysis temperatures (900 °C) by K doping. The formation of light hydrocarbons and light condensables was favoured by bigger par-

ticle size for both pyrolysis temperatures. Light condensable yields were reduced with K doping at both temperatures. Regarding thermochemistry, it has been already discussed that both, K doping and heterogeneous secondary reactions lead to an increase in process exothermicity. We have observed that the combined effect of both phenomena increased further this exothermicity, therefore K doping may favour the presence of these secondary reactions. With this work we aim at contributing to the understanding of the pyrolysis process and to complement other studies towards the further advances in the modelling of the process.

Acknowledgments

References

Almuina-Villar H., Anca-Couce A., Lang N., Röpcke J., Behrendt F., Dieguez-Alonso A., 2018, Laser-based spectroscopy diagnosis and detailed numerical models to gain understanding on the slow pyrolysis behavior of thermally thick wood particles, Chemical Engineering Transactions, 65, 109-114

Almuina-Villar H., Lang N., Anca-Couce A., Röpcke J., Behrendt F., Dieguez-Alonso A., 2019, Application of laser-based diagnosis for characterization of the influence of inorganics on the slow pyrolysis of woody biomass, Journal of Analytical and Applied Pyrolysis, 140, 125-136.

Anca-Couce A., 2016, 'Reaction mechanisms and multi-scale modelling of lignocellulosic biomass pyrolysis', Prog. Energy Combust. Sci. 53, 41–79.

Anca-Couce A., Sommersacher P., Scharler R., 2017, Online experiments and modelling with a detailed reaction scheme of single particle biomass pyrolysis, J. Anal. Appl. Pyrolysis, 127, 411-425.

Demirbaş, A., 2002. Gaseous products from biomass by pyrolysis and gasification: effects of catalyst on hydrogen yield. Energ. Convers. Manage. 43 (7), 897–909.

Di Blasi C., Branca C., Galgano A., 2017, On the Experimental Evidence of Exothermicity in Wood and Biomass Pyrolysis, Energy Technology, 5, 19–29.

Di Blasi C., Branca C., Galgano A., 2018, Role of the Potassium Chemical State in the Global Exothermicity of Wood Pyrolysis, Ind. Eng. Chem. Res., 57, 11561–11571.

Hu S., Jiang L., Wang Y., Su S., Sun L., Xu B., He L., Xiang J., 2015, Effects of inherent alkali and alkaline earth metallic species on biomass pyrolysis at different temperatures, Bioresource Technology, 192, 23-30.

Jakab E., Faix O., Till F., Székely T., 1993, The effect of cations on the thermal decomposition of lignins, Journal of Analytical and Applied Pyrolysis, 25, 185–194.

Jakab E., Faix O., Till F., 1997, Thermal decomposition of milled wood lignin studied by thermogravimetry/mass spectrometry, Journal of Analytical and Applied Pyrolysis, 40-41, 171–186.

Lang N., Rupp C., Almuina-Villar H., Dieguez-Alonso A., Behrendt F., Röpcke J., 2017, Pyrolysis behavior of thermally thick wood particles: Time-resolved characterization with laser based in-situ diagnostics, Fuel, 210, 371-379

Le Brech Y., Ghislain T., Leclerc S., Bouroukba M., Delmotte L., Brosse N., Snape C., Chaimbault P., Dufour A., 2016, Effect of Potassium on the Mechanisms of Biomass Pyrolysis Studied using Complementary Analytical Techniques, ChemSusChem, 9, 863–872.

Patwardhan P. R., Satrio, J.A., Brown R. C., Shanks, B. H., 2010, Influence of inorganic salts on the primary pyrolysis products of cellulose, Bioresource Technology, 101, 4646-4655.

Patwardhan P. R., Brown R. C., Shanks, B. H., 2011, Product Distribution from the Fast Pyrolysis of Hemicellulose, ChemSusChem, 4, 636–643.

Shah M.H., Deng L., Bennadji H. Fisher E. M., 2015, Pyrolysis of Potassium-Doped Wood at the Centimeter and Submillimeter Scales, Energy & Fuels, 29, 7350–7357.

Sommersacher, P., Kienzl, N., Brunner, T., Obernberger, I., 2015, Simultaneous Online Determination of S, Cl, K, Na, Zn, and Pb Release from a Single Particle during Biomass Combustion. Part 1: Experimental Setup-Implementation and Evaluation. Energy and Fuels 29, 6734–6746.

Sommersacher, P., Kienzl, N., Brunner, T., Obernberger, I., 2016, Simultaneous Online Determination of S, Cl, K, Na, Zn, and Pb Release from a Single Particle during Biomass Combustion. Part 2: Results from Test Runs with Spruce and Straw Pellets. Energy and Fuels 30, 3428–3440.

Trendewicz A., Evans, R., Dutta, A., Sykes, R. Carpenter, D., Braun, R., 2015, Evaluating the effect of potassium on cellulose pyrolysis reaction kinetics, Biomass & Bioenergy, 74, 15–25.